Fractional flux lattice and the anyon mean-field approximation

Craig Pryor
Physics Department, University of California, Santa Barbara, California 93106
(Received 25 March 1991; revised manuscript received 5 August 1991)

The anyon mean-field approximation (MFA) is tested by computing the band structure of a charged particle in an infinite two-dimensional square lattice of infinitesimal flux tubes. The band structure and density of states are compared with the MFA and found to be in agreement for $\Phi=1/n$, with $n>3$. For $\Phi=1/2$ and $1/3$, there is no gap, unlike the MFA which predicts a gap. For $\Phi=m/n$ (with $m>1$), there is a gap, opening up the possibility that a superfluid may form for any rational value of the statistical parameter. A physical realization of the $\Phi=1/2$ flux lattice is proposed and a connection between the $\Phi=m/n$ lattice and the fractional quantum Hall effect is discussed.

I. INTRODUCTION

It has been known for a very long time that identical particles fall into two broad categories: fermions and bosons. It has been known for only sightly over a decade, however, that such a division is really a manifestation of our living in three spatial dimensions. In two dimensions there exists the possibility of identical particles characterized by a continuous parameter, which for certain values produces the familiar bosons and fermions, but also interpolates between these two cases.[1-4] Such particles, known as anyons, were originally proposed as mathematical curiosities, but have since been invoked in theories of the quantum Hall effect[5] and high-T_c superconductors,[6] both of which are quasi-two dimensional.

The method used to implement the arbitrary phase for anyon exchange[3] is to exploit the Aharonov-Bohm effect.[7] To each anyon is attached a fictitious charge q, and a fictitious magnetic flux Φ which is confined to an infinitesimally thin tube. The flux produces a vector potential

$$\mathbf{A}(\mathbf{r})=\frac{\Phi}{2\pi}\frac{\hat{\theta}}{r} . \tag{1}$$

For a path in which one particle circles another the phase induced by the Aharonov-Bohm effect is given by

$$\exp(i2a\int d\mathbf{l}\cdot\mathbf{A})=\exp(i2\Phi q) . \tag{2}$$

Here and throughout this paper $\hbar=c=1$. The factor of 2 in Eq. (2) comes about because each charge acquires a phase from the vector potential of the other particle. Since a circling path is equivalent to two exchanges the phase given by Eq. (2) is twice the phase from interchange and we see that by setting $\alpha=q\Phi$ the flux/charge composites acquire a phase of $\exp(i\alpha)$ for paths that interchange particle positions. For $\alpha=0,2\pi,4\pi,\ldots$, the particles are bosons, while for $\alpha=\pi,\ 3\pi,\ldots$, they are fermions.

It is important to keep sight of the fact that $\mathbf{A}(\mathbf{r})$ is purely fictitious and should not have any independent dynamics.[3] If $\mathbf{A}(\mathbf{r})$ were given the dynamics of the real electromagnetic field it would have a finite propagation velocity. This is unacceptable because we wish to assign phases to paths based only on their topology (i.e., the number of times the paths interchange particle positions). We do not want the phase to depend on the distance between the paths, as it would if $\mathbf{A}(\mathbf{r})$ propagated at a finite velocity. In other words, statistics propagate instantaneously. Also, there are no Coulomb interactions between the charges. The charge and flux are completely fictitious and are used only to provide the statistical phase.

Anyons are especially difficult because of the long-range interaction which is made more problematic by its topological nature. One approach to anyon physics has been the mean-field approximation (MFA).[8] The idea is that in a gas any one particle sees the flux due to all the other particles smeared out over the area of the gas. For a number density ρ and statistical parameter $\alpha=q\Phi$ there is an average flux density given by $\rho\Phi$. The MFA consists of replacing this flux density with an effective uniform magnetic field of strength

$$B_{\text{eff}}=\rho\Phi . \tag{3}$$

In this approximation the problem simplifies considerably. The solutions for a spinless particle of charge q in a magnetic field are Landau levels[9] with energy

$$E=(n+\tfrac{1}{2})\omega_c,\quad \omega_c=qB_{\text{eff}}/m . \tag{4}$$

The MFA was the starting point for Laughlin's proposal that an anyon gas spontaneously forms a superfluid.[6] Laughlin noted that if the statistical parameter takes on the value $\alpha=2\pi/l$ for some integer l, then l Landau levels are completely filled. This means that the next available state is ω_c higher in energy and the gap indicates a superfluid. The MFA argument is by no means a proof of superfluidity, although it is a strong indication and other methods indicate a superfluid as well.

There are some nagging questions about the MFA as applied to anyons. Typically an MFA involves averaging

a real magnetic field. For example, in magnetic systems the field at a particular location may be taken to be the average field produced by nearby particles in the system, even though $\mathbf{B}$ varies spatially. Anyons, however, do not actually produce magnetic fields since such fields are confined to the infinitesimally small region inside the flux tube. In fact, the background in which any particular anyon wanders about has $\nabla\times\mathbf{A}(\mathbf{r})=0$, whereas the MFA replaces this with an effective $\mathbf{A}(\mathbf{r})$ for which $\nabla\times\mathbf{A}(\mathbf{r})\neq 0$. One might consider averaging $\mathbf{A}(\mathbf{r})$, instead of $\mathbf{B}$, but the results would be quite different. For a uniform gas there would be as many flux tubes on one side of a particle as on the other. The vector potential would then average to $\mathbf{A}(\mathbf{r})\approx 0$ and we would have a free particle. These arguments are obviously simple-minded, but they point to the uncertainties in how to approximate a gas of anyons. While there is a great deal of experience in dealing with the MFA as applied to systems with real magnetic fields, it is less clear how to handle multiple Aharonov-Bohm scattering.

In this paper we will examine an anyon system that can be solved numerically and compare the results with the predictions of the MFA. In Sec. II the test system, the flux lattice, is introduced and the method used to solve it is discussed. Section III contains the results, and a comparison with the MFA. Finally, in Sec. IV two experimental applications of the flux lattice itself are presented.

II. THE FLUX LATTICE MODEL

The MFA, though appealing in its intuitive simplicity, is not altogether convincing. For the reasons outlined above it is conceivable that some subtlety prevents it from adequately describing the anyon gas. As a test we require a solvable system of anyons involving a large number of particles. An interesting candidate is a system in which all but one of the anyons are held at fixed positions on an infinite square lattice and the remaining particle is free. The MFA is applicable to the system since the fixed anyon flux tubes may be replaced with a uniform B_{eff}. Unlike the anyon gas, however, the single particle in a lattice background can be solved, and the results compared with the MFA. It is also an interesting model by itself since we have a periodic system, but with only Aharonov-Bohm scattering off the "crystal."

This may also be regarded as a different kind of MFA in which flux is distributed throughout the system, but is not smeared outside the flux tubes. The background field is an average from all the other particles, retaining the realistic feature that $\nabla\times\mathbf{A}(\mathbf{r})=0$ everywhere. Using a lattice as a substitute for the MFA has some obvious problems. Not only are the particles constituting the background fixed and thus nondynamical, but there is long-range order as well. However, at a low enough temperature the gas will freeze and develop long-range order anyway. Then a single particle in a fixed lattice background resembles the onset of melting.

The fixed anyon system may be modeled as a free particle with charge q in a square two-dimensional lattice of infinitesimal tubes containing flux Φ. The Hamiltonian is

$$H=\frac{1}{2m}[\mathbf{P}+q\,\mathbf{A}(\mathbf{r})]^2\ , \tag{5}$$

where $\mathbf{A}(r)$ is the vector potential due to all of the flux tubes. The apparent asymmetry between the free charged particle and the fixed flux tubes does not matter since only one particle has any dynamics. The free particle acquires a phase by circling the fixed particles, but the fixed anyons cannot pick up phases from circling one another, so they need not carry charges. This model bears a resemblance to models with periodic magnetic fields.[10,11] The crucial difference is that here $\mathbf{B}=0$ everywhere, although there is a nonzero periodic $\mathbf{A}(\mathbf{r})$.

At this point it is convenient to fix the value of q. Since only $\alpha=\Phi q$ is of concern we may fix the charge q and consider different Φ's. The choice $q=\pi$ is nice because then Φ is in units of flux quanta. For $\Phi=0$ we have bosons and for $\Phi=\frac{1}{2}$ we have "half fermions," particles with statistical parameter midway between bosons and fermions. Throughout this paper the value $q=\pi$ will be used.

Since $\mathbf{A}(\mathbf{r})$ is defined only up to a gauge transformation we must pick a gauge. Rather than requiring $\mathbf{A}(\mathbf{r})$ to satisfy an equation it is more useful to consider particular gauge field configurations which simply give the desired phases. The most convenient gauge for our purposes is known as the singular gauge, in which $\mathbf{A}(\mathbf{r})$ is zero everywhere except along a line extending from the flux tube to infinity, along which

$$\mathbf{A}(\mathbf{r})=\Phi\hat{\mathbf{y}}\delta(y),\quad x>0\ . \tag{6}$$

Here we have taken the flux tube to be at the origin and the phase discontinuity to run along the x axis. In the singular gauge the Aharonov-Bohm phase acquired in going around the flux is contained entirely in the phase discontinuity.

Clearly there is nothing special about a straight line and the phase discontinuity may be deformed in any manner desired, so long as it starts on the flux tube and goes off to infinity. This is advantageous for more than one tube. The discontinuity from one tube can be made to pass through a second tube, after which the two discontinuities are deformed to coincide on their way to the third, and so on. Once the last flux tube has been reached, the discontinuities continue off to infinity together. In this way a system of many flux tubes may be built up so that $\mathbf{A}(\mathbf{r})=0$ everywhere except along a line connecting the flux tubes. For coincident discontinuities the phase is given by the product of the phases from each. Therefore, if the total flux contained in the tubes strung together is an integral multiple of a flux quantum the discontinuity leaving the last tube is the trivial $\mathbf{A}(\mathbf{r})=0$. An example is shown in Fig. 1 in which two flux tubes containing Φ_1 and Φ_2 are joined. If $\Phi_1+\Phi_2=1$, then the discontinuity going off to infinity has the trivial phase 1 which may be omitted.

To compute the flux lattice band structure we assume the wave function to be of the form

$$\psi_{\mathbf{k}}=u_{\mathbf{k}}\exp(i\mathbf{k}\cdot\mathbf{r})\ , \tag{7}$$

where $u_{\mathbf{k}}$ is defined in some unit cell with periodic boundary conditions. The first job is to determine the periodicity of the Hamiltonian, and hence the minimum acceptable unit cell for $u_{\mathbf{k}}$. Naively we might think that the periodicity of the flux tubes reflects the periodicity of the Hamiltonian since a single tube translated by all lattice vectors appears to generate the infinite lattice. However, the Hamiltonian depends on the gauge field $\mathbf{A}(\mathbf{r})$ and we must examine how $\mathbf{A}(\mathbf{r})$ behaves under translations. The behavior of H is determined by the properties of the magnetic group.[12] For the system at hand, however, it is easy to derive the transformation properties of H by exploiting the simplicity of the singular gauge.

First we will show that the unit cell must contain an integer number of flux quanta. Consider the naive unit cell containing only one flux tube, as shown in Fig. 2. With a nonintegral flux the phase discontinuity goes off to infinity, running into the cell boundary. If we try to generate the entire lattice by repeating this unit cell the points where the discontinuities stop at the cell boundaries are sites of phantom flux tubes. A charge circling the intersection of the discontinuity and the boundary will cross the discontinuity only once, thus acquiring a phase. This phase is opposite to that from circling the real flux tube because the discontinuity is crossed in the opposite direction. That is, circling the original flux tube gives $\lambda_{\text{real}}=\exp(i2\pi\Phi)$ while the phantom point at the boundary gives $\lambda_{\text{phantom}}=\exp(-i2\pi\Phi)$. The naive unit cell does not generate the desired lattice but one with extra flux present. Furthermore, since the path of the discontinuity is part of the gauge freedom, the location of the phantom flux tube is not gauge invariant. A different choice of (singular) gauge would give a discontinuity which hit the cell boundary at a different point, resulting in a different phantom lattice.

If the unit cell contains an integral amount of flux the discontinuities may be arranged so as not to run into the cell boundary and the above problem is avoided. Such a unit cell is suitable for computing the band structure, provided that we recognize that the true unit cell is larger still. To see this, consider Fig. 3 in which there are n flux tubes each with flux $\Phi=m/n$. Generating the rest of the lattice requires translating the unit cell, which should be regarded as taking place in the presence of the charged particle. Translating in the $\hat{\mathbf{x}}$ direction, the particle may acquire a phase from crossing one of the discontinuities, with the phase determined by which discontinuity is crossed. Since the phase depends on the positions of the discontinuities, it is gauge dependent. If, however, n copies of such a cell are stacked together the particle crosses n discontinuities and picks up a trivial phase $\exp(i2\pi n/n)$. Therefore, the true unit cell reflecting the translational symmetry of the Hamiltonian is a square with n flux tubes on a side.

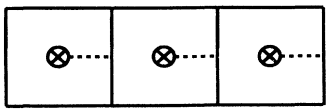

FIG. 2. A unit cell containing a flux tube with a nonintegral amount of flux. In the singular gauge the discontinuity runs into the cell boundary. When the cell is repeated we see a phantom flux tube located at the position where the discontinuity runs into the cell boundary.

The $1\times n$ unit cell will suffice with proper interpretation, which is fortunate since the numerical problem is more formidable for an $n\times n$ cell. The $1\times n$ cell displays a phase change from cell to cell, but this may be absorbed into a redefinition of $\mathbf{k}$ in Eq. (7). Thus, the ambiguity of the $1\times n$ cell only involves an incorrectly defined Brillouin zone. Since we know the true unit cell is $n\times n$, the (incorrect) $1\times n$ unit cell gives a zone which is n times too large in the $\hat{\mathbf{x}}$ direction. We may compute using the $1\times n$ cell, and merely truncate the zone to $1/n$ of its size in the $\hat{\mathbf{x}}$ direction.

Having identified the unit cell, we now turn to the computation of the band structure. Solving Schrödinger's equation for the flux lattice is sightly different from what one usually faces in computing bands. We could do a variational calculation using a set of basis functions, however the phase discontinuities would require us to enforce boundary conditions on the interior of the cell in addition to the periodic boundary conditions already enforced. Furthermore, these interior conditions do not involve simple periodicity, but rather phase relationships. For this reason standard band theory techniques are not well suited.

Instead, our approach is to discretize the unit cell. By using a mesh the Hamiltonian becomes a large sparse matrix which may be numerically diagonalized to find the exact eigenvalues for the discrete system. The eigenvalues of the continuum problem are computed by solving for a series of meshes with progressively finer spacings and extrapolating to the continuum limit. Such a brute

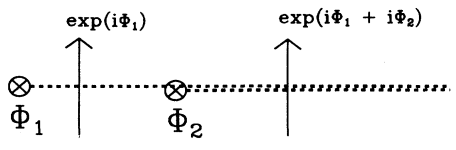

FIG. 1. Two flux tubes Φ_1 and Φ_2 in the singular gauge showing how their phase discontinuities are combined. Phases shown are for a particle with unit charge crossing the direction shown.

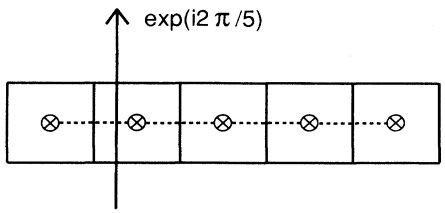

FIG. 3. A unit cell containing 5 $\Phi=\frac{1}{5}$ flux tubes. A particle translated in the $\hat{\mathbf{x}}$ direction can cross a phase discontinuity.

force approach would be unacceptable for most solid state systems because in three dimensions the number of mesh points grows so fast that the Hamiltonian quickly becomes of an unmanageable size. In two dimensions the computations are within reach of a desktop computer. (Before going on we should clear up a potential problem in terminology. The mesh is a *latticization* of the unit cell of a flux *lattice*. To avoid confusion the discretization of the unit cell will always be called a mesh and "lattice" will be reserved for the lattice of flux tubes.)

To construct H_{mn} we must compute the link variables from the distribution of flux tubes, which is quite simple in the singular gauge. Link variables give the phases for going from one site to the next, so only those links traversed by a discontinuity are different from $U=1$. To construct H_{mn} we fix the positions of the flux tubes within the unit cell, connect them with phase discontinuities, check which links are crossed, and assign the appropriate phase to each link.

Before going on to the numerical computations, we note an interesting fact: lattices with flux Φ and $1-\Phi$ have identical energies. Let the matrix H^{Φ}_{mn} denote the Hamiltonian for a lattice of flux tubes Φ. The matrix element connecting sites m and n is

$$H^{\Phi}_{mn} \propto \exp(i2\pi p\Phi) , \tag{8}$$

where p is the number of discontinuities which happen to cross the link connecting sites m and n. Then the Hamiltonian for a flux lattice with flux $-\Phi$ has matrix elements.

$$H^{-\Phi}_{mn} \propto \exp(-i2p\pi\Phi) \tag{9}$$

so that

$$H^{-\Phi}_{mn}=(H^{\Phi}_{mn})^* .$$

But since H_{mn} is Hermitian, the (real) eigenvalues of H_{mn} and H^*_{mn} are the same, and H^{Φ}_{mn} and $H^{-\Phi}_{mn}$ have the same eigenvalues. Clearly the Hamiltonian is periodic in Φ with period 1 since addition of a single flux quantum to each (infinitesimal) flux tube leaves all of the link variables unchanged. Therefore the flux lattices with Φ and $1-\Phi$ have the same energies. This is something of a help since it means that there are only half as many computations to do.

III. BAND STRUCTURE

Some of the results of the numerical calculations are shown in Figs. 4–13. Altogether 18 different flux lattices were considered with $\Phi=m/n$ for denominators running from 2 to 9, and with $\Phi=\frac{2}{11}$, $\frac{3}{11}$, $\frac{4}{11}$, and $\frac{5}{11}$. Lattices with $m/n>\frac{1}{2}$ were ignored since they are identical to those with $\Phi=1-m/n$, as shown in the previous section. All diagrams use $1/(ma^2)$ as the unit of energy, where a is the spacing between flux tubes and all states are counted in units of states/(flux tube) rather than states/(flux quantum). The corresponding graphs obtained by the MFA are indicated by dotted lines.

Along each direction in the Brillouin zone energy levels were calculated at 10 evenly spaced values of $\mathbf{k}$ to obtain the band diagrams. Energies were computed by diagonalizing four matrix Hamiltonians with 7, 9, 11, and 13 mesh sites per side of a square containing one flux tube. The unit cell contained n such squares, stacked together as in Fig. 3. Eigenvalues were computed using the Lanczos algorithm.[13] The continuum energies were found by extrapolating the energies as a function of mesh spacing with a polynomial fit to the four eigenvalues.[14] The density of states (DOS) was calculated by first computing energies on a 10×10 grid within the Brillouin zone, then using a two-dimensional polynomial interpolation to compute energies at points on a 500×500 square grid in $\mathbf{k}$ space. The energies were counted in 300 bins and normalized to give states/(flux tube).

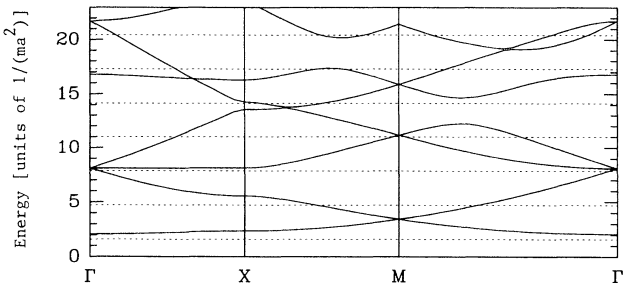

FIG. 4. Band diagram for $\Phi=\frac{1}{2}$.

In Fig. 4 we see the bands for $\Phi=\frac{1}{2}$, corresponding to half fermions. The key feature is the absence of an energy gap. The lowest and second lowest bands meet at the M point, in contrast to the MFA prediction of a gap. In general, the agreement with the MFA is rather poor. While the lowest band is flat throughout most but not all of the zone, many of the higher bands look like shifted free particle dispersion relations. The relative flatness of the lowest band and the near gap at the M point is made very clear in the DOS, shown in Fig. 5. That the lowest band is flat throughout most of the zone is demonstrated by the narrow low-energy peak in the DOS. The $\Phi=\frac{1}{2}$ flux lattice appears to be on the edge of agreement with the MFA, at least so far as an energy gap is concerned. There is some correlation between the MFA and the flux

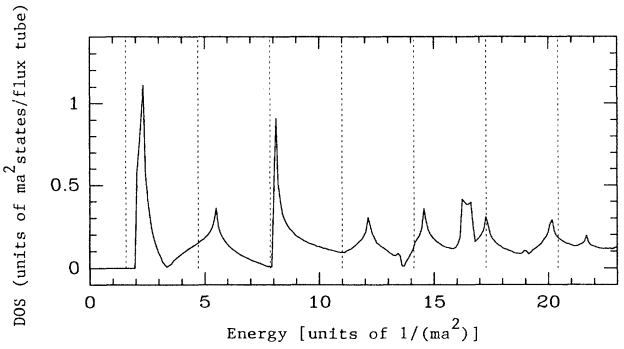

FIG. 5. DOS for $\Phi=\frac{1}{2}$.

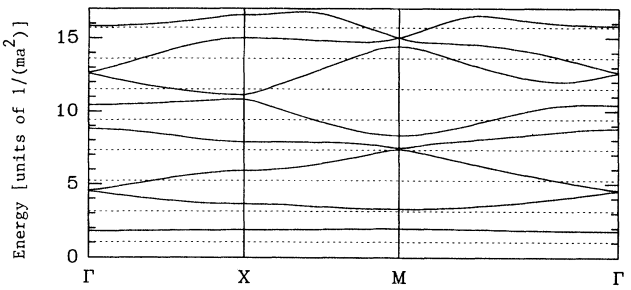

FIG. 6. Band diagram for $\Phi=\frac{1}{3}$.

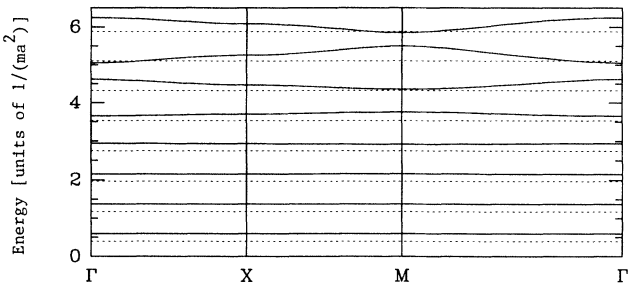

FIG. 8. Band diagram for $\Phi=\frac{1}{8}$.

lattice in that the spacing of the DOS peaks is about equal to the Landau level spacing. The failure of the MFA is interesting because $\Phi=\frac{1}{2}$ is the simplest nontrivial case and if a gap were generic for any value of α we would expect a gap here.

For $\Phi=\frac{1}{3}$ the agreement with the MFA improves slightly. Figure 6 shows that a gap between the first and second bands has opened up at the M point. Some of the curvature seen for $\Phi=\frac{1}{2}$ is present, especially in the higher bands, but the lowest band looks very much like a flat Landau level. The DOS shows a clear gap above the lowest-lying band, followed by a series of "near gaps," much like those seen for $\Phi=\frac{1}{2}$. The presence of a gap above the lowest band does not quite confirm the MFA, however, since the MFA requires self-consistent filling. Each band contains a total of $\frac{1}{3}$ states/(flux tube), so the MFA requires that we fill the first three bands. The third and fourth bands touch at the M point and the MFA fails by predicting a nonexistent gap.

As we proceed though lattices with $\Phi=1/n$ there is a clear progression toward flat, evenly spaced bands, and for $\Phi<\frac{1}{3}$ there is a gap at self-consistent filling. The energies lie above the corresponding Landau level energies, though they approach the Landau levels as n gets larger. Despite the upward shift in energy over the MFA prediction, the spacing between bands matches the MFA prediction very well. Also, the higher-lying curved bands still give pronounced peaks in the DOS. The bands and DOS shown in Figs. 8 and 9 show the good agreement with the MFA for $\Phi=\frac{1}{8}$.

We now turn to lattices with $\Phi=m/n$, with $m>1$. For these lattices the complicated band structure makes it more illuminating to look at the integrated DOS (IDOS). Since this counts the number of states below a given energy, steep rises indicate peaks in the DOS (approximate Landau levels), while plateaus indicate energy gaps. The IDOS for $\Phi=\frac{2}{11}$ and $\frac{5}{11}$ are shown in Figs. 10 and 11. The $m/11$ lattices were chosen to best show the effect of increasing the numerator. Other denominators show the same qualitative features.

In all cases the lowest m bands are very closely spaced, appearing in the IDOS as m nearby steps. In a few cases the bands are so closely spaced that they look like a single degenerate band, although the energies are numerically distinct. Each MFA Landau level contains m/n states per flux tube. For the flux lattice the corresponding Landau level is actually composed of m closely spaced levels, each containing $1/n$ states per flux tube.

At low energies the levels containing $1/n$ states are clustered into groups of m levels, giving the appearance of an MFA Landau level with m/n states. At higher energies there are still steps in the IDOS, but they appear at energy spacings corresponding to $\Phi=1/n$, not $\Phi=m/n$. That is, they are spaced at fractions $1/m$ of an MFA Landau level. The energy at which the $1/n$ steps become pronounced is indicated by the size of m/n. Agreement with the MFA persists to higher energies for smaller m/n. For $\Phi=\frac{2}{11}$ the low-lying states look much like

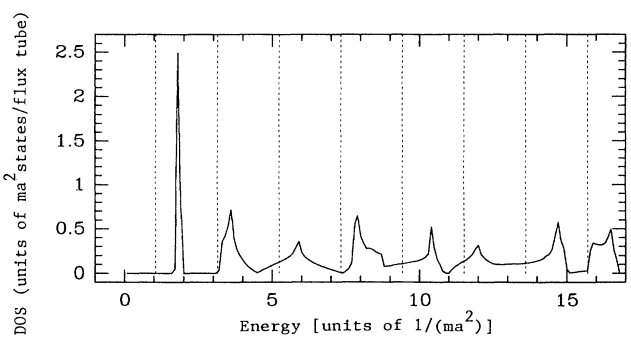

FIG. 7. DOS for $\Phi=\frac{1}{3}$.

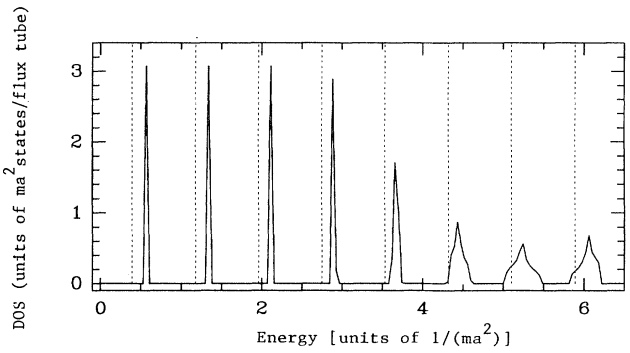

FIG. 9. DOS for $\Phi=\frac{1}{8}$.

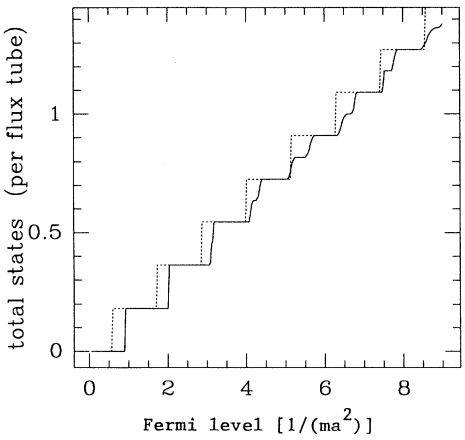

FIG. 10. Integrated DOS for $\Phi=\frac{2}{11}$.

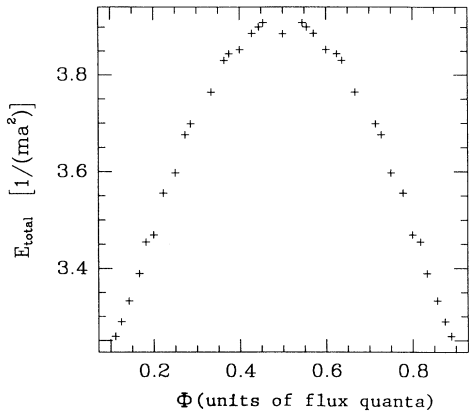

FIG. 12. Total energy per particle for self-consistent filling as a function of flux.

MFA Landau levels, only to break into $1/n$ type Landau levels after the first few m/n type steps. On the other hand, for $\Phi=\frac{5}{11}$ even the first step is broken into five closely spaced steps. As a consequence of the $1/n$ spacing all of the m/n lattices have an energy plateau at a filling of one state per flux tube. This result differs markedly from the MFA, which predicts that at self-consistent filling the highest occupied Landau level is partially filled, producing no gap. Instead the m/n lattices do have a gap at self-consistent filling, a feature completely missed by the MFA.

An interesting quantity to examine is the total energy of a flux lattice with states filled up to 1 state/flux tube. This is plotted in Fig. 12 as a function of flux, with $\Phi>\frac{1}{2}$ included. The total energies are fairly regular in their dependence on Φ, with only slight scatter about a smooth curve. Only for $\Phi=\frac{1}{2}$ is there much deviation from the smooth curve, which is attributable to the fact that $\Phi=\frac{1}{2}$ is gapless. It should be noted that $\Phi=\frac{1}{3}$ has no gap at the Fermi level, although it has a gap between the first and second bands. This explains why its total energy is not anomalous like that for $\Phi=\frac{1}{2}$, since the filled states are approximate Landau levels.

The energy gaps at the Fermi level for self-consistent filling, shown in Fig. 13, are less systematic in their dependence on Φ. Nonetheless, the gaps for m/n lattices are comparable to those for $1/n$. In fact, for the $\frac{2}{5}$, $\frac{3}{7}$, and $\frac{4}{9}$ lattices the gaps are considerably larger than any of the $1/n$ lattices. The gaps are more systematic if one considers a fixed denominator. For a given n the gap at self-consistent filling increases with m, and it seems reasonable to postulate that as $m/n\rightarrow\frac{1}{2}$ the gap widens, although at $m/n=\frac{1}{2}$ there is no gap.

In summary, the MFA and the flux lattice are in qualitative agreement for $\Phi=1/n<3$. The spacings between levels agree with the MFA remarkably well. For all $\Phi=1/n<\frac{1}{3}$ there is a gap at the Fermi level for a filling of 1 state/(flux tube). The states for $\Phi=m/n$ agree with the MFA only for the lowest few Landau levels. For higher energies approximate Landau levels occur at spac-

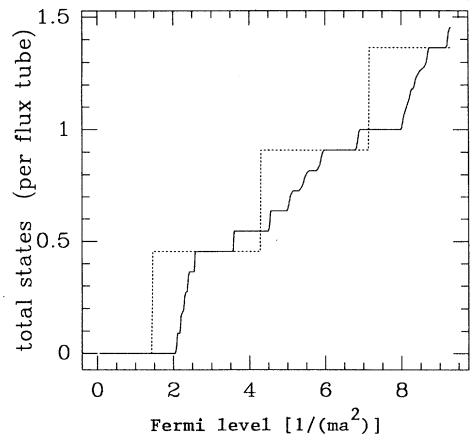

FIG. 11. Integrated DOS for $\Phi=\frac{5}{11}$.

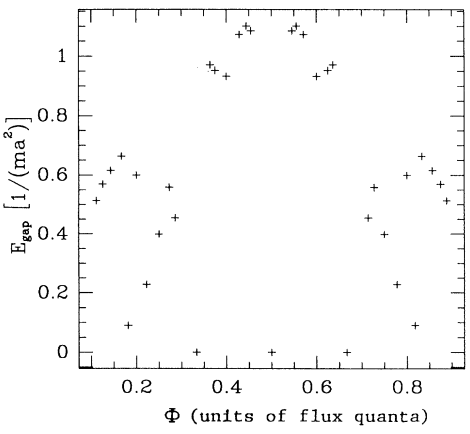

FIG. 13. Energy gap at the Fermi surface for self-consistent filling as a function of flux.

ings corresponding to $1/m$ of the energy predicted by the MFA. This leads to an energy gap at 1 particle per flux tube that is not seen in the MFA. Therefore, all the flux lattices have gaps at 1 particle per flux tube, not just those with $\Phi=1/n$. This surprising result demonstrates that confining flux to tubes gives energy levels which are qualitatively different from those for a uniform field. If we regard the flux lattice as a new MFA in which flux tubes are uniformly distributed rather than flux itself, we would be led to the conclusion that any $\alpha=\pi m/n$ gives rise to a superfluid. Whether or not this feature is spoiled by giving dynamics to the background particles is an open question.

IV. EXPERIMENTAL CONSEQUENCES

Beyond its implications for the anyon MFA the flux lattice may have other applications, two of which will be considered here. First, we will examine the possibility of actually manufacturing a flux lattice. We will then examine some of the similarities between the flux lattice and the fractional quantum Hall effect.

The most familiar flux lattice is the Abrikosov lattice,[15] formed by the flux which penetrates a type-II superconductor placed in a magnetic field. Unlike the lattices considered in this paper, the Abrikosov lattice is composed of tubes containing one flux quantum, given by $\Phi_{II}=\pi/e$. To obtain a lattice of fractional flux we may exploit the fact that the flux quantum in an ordinary conductor is $2\Phi_{II}$, since the charge carriers are single electrons rather than Cooper pairs. If a quasi-two-dimensional electron gas in close proximity to a layer of type-II superconductor were placed in a magnetic field, the flux tubes coming out of the superconductor would contain Φ_{II}, which is $\frac{1}{2}$ the flux quantum for the electron gas. This provides a physical realization of the $\Phi=\frac{1}{2}$ flux lattice.

Abrikosov flux tubes are typically on the order of 10^{-5} cm in diameter, with a somewhat larger spacing between flux tubes.[16] This means that in order to minimize the divergence of the flux once it leaves the superconductor the electron gas thickness and distance to the superconducting layer must be less than 10^{-5} cm. Such a structure could be fabricated using a GaAs quantum well with thin AlAs barriers, upon which would be deposited a layer of superconductor. An additional requirement is that the quantum well have sufficiently high mobility that the coherence length is longer than the flux tube spacing. Since coherence lengths of 100 μm are achievable[17] this is no problem.

An obvious difference between such an arrangement and the $\Phi=\frac{1}{2}$ lattice considered in Sec. II is that the Abrikosov lattice is hexagonal. This is a minor inconvenience, however, as only the fine details of the band structure will change. More serious are the departures from ideal flux tubes. Not only do real flux tubes have a nonzero cross section, but the electrons are not excluded from the interior of the tube. A possible remedy is to use a focused ion beam to make a lattice of damaged spots.[18] If this was done to the complete superconductor-semiconductor system the dots would be aligned in both layers. The damaged areas of the superconductor would pin the flux tubes, while the damaged regions of the electron gas would exclude the electrons from the flux tube interior. An added benefit is that the flux tubes could be arranged in any desired lattice. Damage will, however, reduce the coherence length in the electron gas by a factor of ≈ 300, possibly making the undamaged version more useful.[18]

Construction of a real flux lattice seems limited to $\Phi=\frac{1}{2}$. To explore other values of flux we may take a more indirect approach. There is an intriguing similarity between the $\Phi=m/n$ flux lattices and the fractional quantum Hall effect (FQHE). In the FQHE there are energetically favorable states when a rational fraction of a Landau level is filled. Similarly, for the $\Phi=m/n$ flux lattices the MFA predicts Landau levels, while the calculations show that when a fraction p/m of a MFA Landau level is filled there is a gap to the next available state. The size of the gap depends on the arbitrary integer p, and which Landau level is being filled. Therefore, if the applied magnetic field in the FQHE were represented as $\Phi=m/n$ flux tubes, then the stability at fractional filling would follow from the results for the flux lattice. That is, with a uniform magnetic field we find energy gaps with Landau level spacing, while if the field is concentrated into flux tubes with $\Phi=m/n$ we find new energy gaps when p/m of a Landau level is filled.

The similarity is suggestive, but there are differences to recognize. In the flux lattice the filling fractions at which gaps appear are p/m, and since m can be anything at all any fraction is possible. The FQHE, however, usually shows gaps at fractions with odd denominators, with even denominators appearing only under extreme conditions of high magnetic field. Since even denominators are believed to be associated with the electron's spin, they should not appear in a spinless treatment of the problem.

Another difficulty is that there is no apparent reason for the flux from the uniform field to fragment into fractional flux tubes. The total energy for the flux lattice filled to some Fermi level is higher than for a uniform magnetic field with the same filling. This indicates that the uniform field states are energetically favored over the fractional flux states represented by the flux lattice. Examination of the total energy versus Fermi level shows this to be true for all the flux lattices considered. If some way could be found to make the fractional flux state stable, or even metastable, there might be interesting consequences.

Since the results of Sec. II depend only on the product $q\Phi$, a fractional charge would produce identical results in the presence of tubes containing one flux quantum. Since the quasiparticles in the FQHE do indeed carry fractional charge, the connection between the flux lattice and the FQHE may involve the fractional charged quasiparticles rather than fractional flux.

ACKNOWLEDGMENT

I wish to thank Frank Wilczek for helpful discussions.

[1]J. M. Leinass and J. Myrheim, Nuovo Cimento **37B**, (1977).
[2]G. A. Goldin, R. Menikoff, and D. H. Sharp, J. Math. Phys. **21**, 650 (1980); **22**, 1664 (1981).
[3]F. Wilczek, Phys. Rev. Lett. **49**, 957 (1982).
[4]F. Wilczek and A. Zee, Phys. Rev. Lett. **51**, 2250 (1983).
[5]B. I. Halperin, Phys. Rev. Lett. **52**, 1583, 2390(E) (1984).
[6]R. Laughlin, Phys. Rev. Lett. **60**, 2677 (1988).
[7]Y. Aharonov and D. Bohm, Phys. Rev. **188**, 1139 (1959).
[8]D. Arovas, R. Schrieffer, F. Wilczek, and A. Zee, Nucl. Phys. **B251**, 117 (1985).
[9]L. D. Landau and E. M. Lifshitz, *Quantum Mechanics* (Pergamon, London, 1977).
[10]D. Hofstadter, Phys. Rev. B **14**, 2239 (1976).
[11]S. P. Novikov, Sov. Math. Dokl. **23**, 298 (1981).
[12]J. Zak, Phys. Rev. **134**, A1602 (1964).
[13]C. Lanczos, J. Res. Natl. Bur. Stand. Sec. B **45**, 255 (1950); J. Cullum and R. A. Willoughby, J. Comput. Phys. **44**, 329 (1981).
[14]W. H. Press, B. P. Flannery, S. A. Teukolsky, and W. T. Vetterling, *Numerical Recipes* (Cambridge University Press, England, 1986).
[15]A. A. Abrikosov, Zh. Eksp. Teor. Fiz. **32**, 1442 (1957) [Sov. Phys. JETP **5**, 1174 (1957)].
[16]W. A. Harrison, *Solid State Theory* (Dover, New York, 1972).
[17]J. Spector *et al.*, Surf. Sci. **228**, 283 (1990).
[18]K. Enslin and P. M. Petrov, Phys. Rev. B **41**, 12 307 (1990).